J|A|C|S ARTICLES

Published on Web 05/06/2010

Circular Dichroism Tensor of a Triarylmethyl Propeller in Sodium Chlorate Crystals

Yonghong Bing,[†] David Selassie,[†] Ruthanne H. Paradise,[‡] Christine Isborn,[†,§] Nicholas Kramer,[†] Martin Sadilek,[†] Werner Kaminsky,*[,†] and Bart Kahr*[,‡]

Department of Chemistry, University of Washington, Box 351700, Seattle, Washington 98195, and Department of Chemistry and Molecular Design Institute, New York University, New York, New York 10003

Received March 5, 2010; E-mail: wernerka@u.washington.edu; bart.kahr@nyu.edu

Abstract: In 1919, Perucca reported anomalous optical rotatory dispersion from chiral $NaClO_3$ crystals that were colored by having been grown from a solution containing an equilibrium racemic mixture of a triarylmethane dye (Perucca, E. *Nuovo Cimento* **1919**, *18*, 112−154). Perucca's chiroptical observations are apparently consistent with a resolution of the propeller-shaped dye molecules by $NaClO_3$ crystals. This implies that Perucca achieved the first enantioselective adsorption of a racemic mixture on an inorganic crystal, providing evidence of the resolution of a triarylmethyl propeller compound lacking bulky ortho substituents. Following the earlier report, $NaClO_3$ crystals dyed with aniline blue are described herein. The rich linear optical properties of (001), (110), and (111) sections of these mixed crystals are described via their absorbance spectra in polarized light as well as images related to linear dichroism, linear birefringence, circular dichroism, and anomalous circular extinction. The linear dichroism fixes the transition electric dipole moments in the aromatic plane with respect to the growth faces of the $NaClO_3$ cubes. Likewise, circular dichroism measurements of four orientations of aniline blue in $NaClO_3$ fix a bisignate tensor with respect to the crystal growth faces. Electronic transition moments and circular dichroism tensors were computed ab initio for aniline blue. These calculations, in conjunction with the crystal-optical properties, establish a consistent mixed-crystal model. The nature of the circular extinction depends upon the crystallographic direction along which the crystals are examined. Along ⟨100⟩, the crystals evidence circular dichroism. Along ⟨110⟩, the crystals evidence mainly anomalous circular extinction. These two properties, while measured by the differential transmission of left and right circularly polarized light, are easily distinguished in their transformation properties with respect to reorientations of the sample plates. Circular dichroism is symmetric with respect to the wave vector, whereas anomalous circular extinction is antisymmetric. Analysis of Perucca's raw data reveals that he was observing a convolution of linear and circular optical properties. The relatively large circular dichroism should in principle establish the absolute configuration of the propeller-shaped molecules associated with *d*- or *l*-$NaClO_3$ crystals. However, this determination was not as straightforward as it appeared at the outset. In the solid state, unlike in solution, a strong chiroptical response is not in and of itself evidence of enantiomeric resolution. It is shown how it is possible to have a poor resolution—even an equal population of *P* and *M* propellers—within a given chiral $NaClO_3$ crystal and still have a large circular dichroism.

Introduction

We know virtually nothing by *experiment* about the orientational dependence of the optical rotation and circular dichroism in molecules;[1,2] this is a hole in the science of molecular chirality as well as an opportunity. One of several motivations for systematically studying the process of dyeing crystals[3] was to prepare a class of materials with colored sublattices having only translational symmetry that could be subject to measurements of the anisotropy of circular dichroism. This plan was thwarted because dyed anisotropic crystals, we discovered, are often dominated by the differential absorption of left and right circularly polarized light that arises when embedded oscillators adopt biased orientations with respect to the eigenmodes of the medium. We called this effect anomalous circular extinction (ACE).[4] To obviate the ACE effect, we could resort to a chiral optically isotropic host such as $NaClO_3$.[5] Unfortunately, $NaClO_3$ is difficult to dope with optically responsive molecules.[3]

[†] University of Washington.
[‡] New York University.
[§] Present address: Department of Chemistry, Stanford University, Stanford, CA 94305.

(1) Kuball, H.-G.; Höfer, T. In *Circular Dichroism: Principles and Applications*, 2nd ed; Berova, N., Nakanishi, K., Woody, R. W., Eds.; Wiley-VCH: Weinheim, Germany, 2000; pp 133−158. Kuball, H.-G. *Enantiomer* **2002**, *7*, 197–205.
(2) Claborn, K.; Herreros Cedres, J.; Isborn, C.; Zozulya, A.; Weckert, E.; Kaminsky, W.; Kahr, B. *J. Am. Chem. Soc.* **2006**, *128*, 14746–14747. Claborn, K.; Isborn, C.; Kaminsky, W.; Kahr, B. *Angew. Chem., Int. Ed.* **2008**, *47*, 5706–5717.
(3) Kahr, B.; Gurney, R. W. *Chem. Rev.* **2001**, *101*, 893–951.
(4) Kaminsky, W.; Herreros Cedres, J.; Geday, M. A.; Kahr, B. *Chirality* **2004**, *16*, S55–S61. Claborn, K.; Chu, A.-S.; Jang, S.-H.; Su, F.; Kaminsky, W.; Kahr, B. *Cryst. Growth Des.* **2005**, *5*, 2117–2123.

10.1021/ja1018892

However, there exists in the literature a description of a $NaClO_3$ crystal that had been treated with a textile dye during growth from solution.[6] Herein we present an analysis of the rich optical properties of this crystal using a variety of differential polarization imaging techniques[7] that limns what we can and cannot determine from such crystals using polarized light.

The mixed crystal in question was prepared in 1919 by Perucca,[8] who reported anomalous optical rotatory dispersion (ORD) from chiral $NaClO_3$ crystals that were colored by having been grown from a solution containing an equilibrium racemic mixture of a triarylmethane dye, extra China blue.[6] Perucca's chiroptical observations, which were mentioned in Mellor's classic treatise on inorganic chemistry,[9] are apparently consistent with the resolution of the propeller-shaped dye molecules by $NaClO_3$ crystals. If substantiated, this would be the first evidence of enantioselective adsorption of a racemic mixture on an inorganic crystal.[10] Stereochemical investigations of this kind failed to find fertile ground until the 1970s, when crystal−molecule interactions took a prominent place in discussions of the origin of biomolecular homochirality.[11]

Discrimination of enantiomers by minerals[12,13] has been a subject of speculation since the first suggestions that quartz or chiral clays may have been responsible for biochirogenesis.[14,15] Since 1935, many scientists claimed to have resolved racemates with *d*- or *l*-quartz powders,[16] but their observations of residual optical activities were later deemed to be experimentally insignificant.[17,18] Ferroni and Cini[19] even claimed to have resolved optical antipodes with $NaClO_3$, although they appeared to be unaware of Perucca's paper.[6] Their work was discredited,[20] as were the earlier quartz studies.[16] The 19th century observation that D-glucose as a cosolute biases the handedness of $NaClO_3$ crystals,[21] which was presumed to be evidence of enantioselectivity, has not stood up to a contemporary reinvestigation.[22] Bonner et al.[23] ultimately collected reliable data on asymmetric adsorption on quartz in 1974, and their work is generally considered to be a milestone. Researchers have subsequently described many enantioselective processes on crystal surfaces.[3,13,24] The autocatalytic Soai reaction has given abundant evidence of enantioselective adsorption on a variety of crystals,[25,26] including $NaClO_3$.[27,28] Perucca's paper[6] on anomalous ORD from dyed $NaClO_3$ antedates all claims to have resolved racemic mixtures with chiral crystals. In our view, it is a significant work in the history of molecular chirality, and for this reason we have subjected it to a thorough reinvestigation.

Crystal Growth and Sample Preparation

We identified aniline blue (**1**) as the compound most akin to extra China blue whose constitution Perucca qualified as *probabilmente*.[29] Specifically, Perucca identified the active colored component as *trifenil-triparaamido-di/trifenil-tolil-carbinolo-di/monosolfonato di Na o di(NH$_4$): $C_{37/38}H_{28/29}N_3(SO_3)_{1/2}(Na_{1/2})$*.[30] In solution, λ_{max} of Perucca's extra China blue was 588 nm (concentration unspecified). The λ_{max} of commercial **1** (diammonium salt, Aldrich, CI no. 42780, CAS no. 66687-07-8) fell from 600 to 590 nm as the solution concentration was increased from 1.2×10^{-4} to 7.6×10^{-4} M. The extinction coefficient in water was 4.0×10^4 M^{-1} cm^{-1}.

Historically, commercial aniline blue has principally been a mixture of two compounds,[29] acid blue 93 (CAS no. 28983-56-4)[31] and acid blue 22 (CAS no. 28631-66-5)[32] (Scheme 1). However, the Aldrich sample contained no trace of acid blue 22, as determined by ion-trap mass spectrometry in the positive-ion mode. The major ion was found at *m*/*z* 756, consistent with trisulfonated acid blue 93. In smaller abundance were disulfonated (*m*/*z* 676) and tetrasulfonated (*m*/*z* 836) analogues. The mixture was separated on silica (200−400 mesh, 1:1 ethanol/methylene chloride) into two colored bands, a blue band and a more rapidly eluting purple band. The blue band contained the tri- and tetrasulfonates, while the purple band contained the

(5) Gopalan, P.; Peterson, M. L.; Crundwell, G.; Kahr, B. *J. Am. Chem. Soc.* **1993**, *115*, 3366–3367. Gopalan, P.; Crundwell, G.; Bakulin, A.; Peterson, M. L.; Kahr, B. *Acta Crystallogr.* **1997**, *B53*, 189–202. Shtukenberg, A. G.; Rozhdestvenskaya, I. V.; Popov, D. Y.; Punin, Y. O. *J. Solid State Chem.* **2004**, *177*, 4732–4742.

(6) Perucca, E. *Nuovo Cimento* **1919**, *18*, 112–154.

(7) Kaminsky, W.; Claborn, K.; Kahr, B. *Chem. Soc. Rev.* **2004**, *33*, 514–525.

(8) Perucca was a colorful character. For more about him, see: Kahr, B.; Bing, Y.; Kaminsky, W.; Viterbo, D. *Angew. Chem., Int. Ed.* **2009**, *48*, 3744–3748. Jacoby, M. *Chem. Eng. News* **2008**, *86* (33), 38–41.

(9) Mellor, J. W. *A Comprehensive Treatise on Inorganic and Theoretical Chemistry*; Longmans, Green and Co.: London, 1922; Vol. II, p 325.

(10) Kahr, B.; Chittenden, B.; Rohl, A. *Chirality* **2005**, *18*, 127–133.

(11) Bonner, W. A.; Kavasmaneck, P. R.; Martin, F. S.; Flores, J. J. *Origins Life Evol. Biospheres* **1975**, *6*, 367–376. Mason, S. *Chem. Soc. Rev.* **1988**, *17*, 347–359. Feringa, B. F.; van Delden, R. A. *Angew. Chem., Int. Ed.* **1999**, *38*, 3418–3438. Cintas, P. *Angew. Chem., Int. Ed.* **2002**, *41*, 1139–1145.

(12) Bondy, S. C.; Harrington, M. E. *Science* **1979**, *203*, 1243–1244. Cody, A. M.; Cody, R. D. *J. Cryst. Growth* **1991**, *113*, 508–519. Orme, C. A.; Noy, A.; Wierzbicki, A.; McBride, M. T.; Grantham, M.; Teng, H. H.; Dove, P. M.; DeYoreo, J. J. *Nature* **2001**, *411*, 775–779. Addadi, L.; Geva, M. *CrystEngComm* **2003**, 140–146. Downs, R. T.; Hazen, R. M. *J. Mol. Catal. A: Chem.* **2004**, *216*, 273–285.

(13) Hazen, R. M.; Sholl, D. S. *Nat. Mater.* **2003**, *2*, 367–374.

(14) Goldschmidt, V. M. *New Biol.* **1952**, *12*, 97–105.

(15) Bernal, J. D. *The Physical Basis of Life*; Routledge and Paul: London, 1951.

(16) Tsuchida, R.; Kobayashi, M.; Nakamura, A. *J. Chem. Soc. Jpn.* **1935**, *56*, 1339–1345. Karagunis, G.; Coumoulos, G. *Nature* **1938**, *142*, 162–163. Bailar, J. C., Jr.; Peppard, D. F. *J. Am. Chem. Soc.* **1940**, *62*, 105–109. Terent'ev, A. P.; Klabunovskii, E. I.; Patrikeev, V. V. *Dokl. Akad. Nauk SSSR* **1950**, *74*, 947–950.

(17) Amariglio, A.; Amariglio, H.; Duval, X. *Helv. Chim. Acta* **1968**, *51*, 2110–2132.

(18) For an excellent review of enantioselective adsorption to quartz, see: Bonner, W. A. In *Exobiology*; Ponnamperuma, C. P., Ed.; North Holland: Amsterdam, 1972; pp 170−234.

(19) Ferroni, E.; Cini, R. *J. Am. Chem. Soc.* **1960**, *82*, 2427–2428.

(20) Gillard, R. D.; da Luz de Jesus, J. D. P. *J. Chem. Soc., Dalton Trans.* **1979**, 1779–1782.

(21) Kipping, F. S.; Pope, W. J. *Trans. Chem. Soc.* **1898**, *73*, 606–617.

(22) Alexander, A. J. *Cryst. Growth Des.* **2008**, *8*, 2630–2632.

(23) Bonner, W. A.; Kavasmaneck, P. R.; Martin, F. S.; Flores, J. J. *Science* **1974**, *186*, 143–144.

(24) Addadi, L.; Berkovitch-Yellin, Z.; Weissbuch, I.; Lahav, M.; Leiserowitz, L. *Top. Stereochem.* **1986**, *16*, 1–85. Weissbuch, I.; Popovitz-Biro, R.; Lahav, M.; Leiserowitz, L. *Acta Crystallogr.* **1995**, *B51*, 115–148.

(25) Kahr, B.; Lovell, S.; Subramony, J. A. *Chirality* **1998**, *10*, 66–77. Gurney, R. W.; Mitchell, C. A.; Ham, S.; Bastin, L. D.; Kahr, B. *J. Phys. Chem. B* **2000**, *104*, 878–892.

(26) Soai, K.; Osanai, S.; Kadowaki, K.; Yonekubo, S.; Shibata, T.; Sato, I. *J. Am. Chem. Soc.* **1999**, *121*, 11235–11236. Sato, I.; Kadowaki, K.; Urabe, H.; Jung, J. H.; Ono, Y.; Shinkai, S.; Soai, K. *Tetrahedron Lett.* **2003**, *44*, 721–724. Kawasaki, T.; Suzuki, K.; Hatase, K.; Otsuka, M.; Koshima, H.; Soai, K. *Chem. Commun.* **2006**, 1869–1871.

(27) Sato, I.; Kadowaki, K.; Soai, K. *Angew. Chem., Int. Ed.* **2000**, *39*, 1510–1512. Soai, K.; Sato, I. *Chirality* **2002**, *14*, 548–554. Sato, I.; Kadowaki, K.; Ohgo, Y.; Soai, K. *J. Mol. Catal. A: Chem.* **2004**, *216*, 209–214.

(28) Pagni, R. M.; Compton, R. N. *Cryst. Growth Des.* **2002**, *2*, 249–253.

(29) Green, F. J. *The Sigma-Aldrich Handbook of Stains, Dyes, and Indicators*; Aldrich Chemical Co.: New York, 1990; pp 96−97. For difficulties establishing the constitutions of old commercial dyes, see: Kelley, M. P.; Chow, J. K.; Kahr, B. *Mol. Cryst. Liq. Cryst.* **1994**, *242*, 201–214.

(30) In a footnote, Perucca says that "bleu d'anilina" did *not* color the crystals (see p 123 in ref 2).

(31) Also called methyl blue. CI no. 42780 is sometimes associated with a mixture and sometimes associated with a pure component, acid blue 93.

Scheme 1

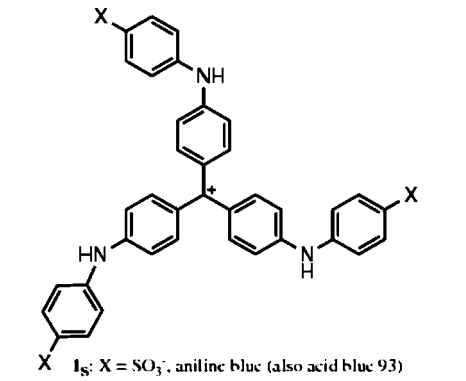

1_S: X = SO_3^-, aniline blue (also acid blue 93)
3_S: X = H

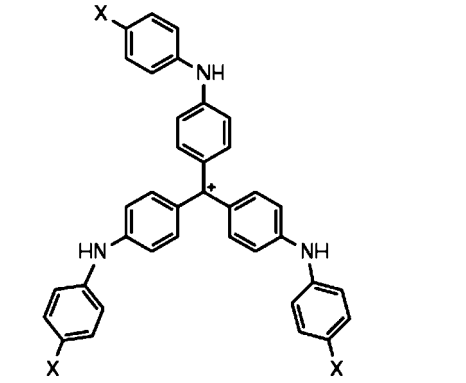

1_A: X = SO_3^-, aniline blue - asymmetric conformation
3_A: X = H

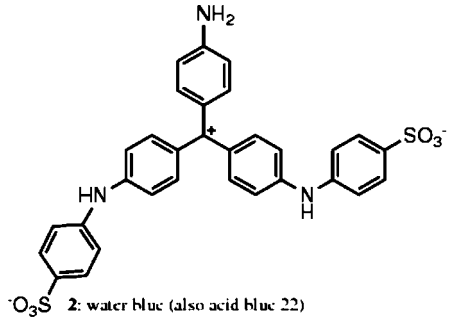

2: water blue (also acid blue 22)

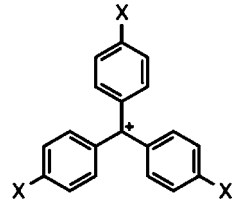

4: X = $N(CH_3)_2$
5: X = H, triphenylmethyl cation

disulfonate. Curiously, when the purified fractions were used to grow crystals of $NaClO_3$, the dyes precipitated from the growth solutions. The mixed crystals were prepared only from the untreated Aldrich sample. The dye mixtures were surprisingly more soluble than either of the purified fractions, which proved to be good fortune essential to carrying out the experiments described herein. For the blue fraction, $\lambda_{max} = 584$ nm at 1.2×10^{-4} M in water, as compared with 590 nm for the commercial mixture. For the purple fraction, $\lambda_{max} = 560$ nm. The blue fraction showed a modest blue shift from 584 to 560 nm upon saturation of aqueous solutions with $NaClO_3$; this was quite distinct from the mixture, which shifted from 590 to 545 nm.

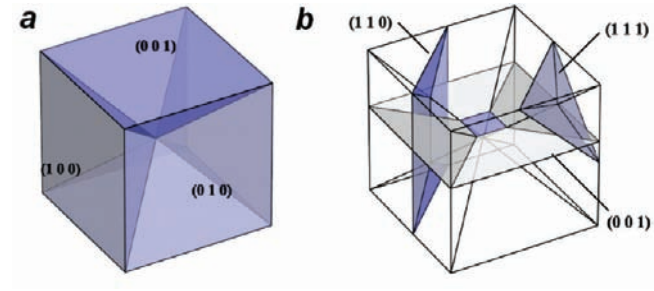

Figure 1. (a) Idealized cube separated into six growth pyramids or sectors. Distinct colors indicate that adjacent sectors are not related to one another by rotations parallel to any principal direction. (b) (001), (110), and (111) sections excised from crystals for spectroscopic and microscopic examination. Shading indicates that distinct tiles within any section correspond to unique optical orientations with respect to the section. {001} sections have twofold symmetry. {110} sections are asymmetric. {111} sections are threefold-symmetric.

Crystals of $NaClO_3$ were grown at room temperature and at 5 °C in a refrigerator by slow evaporation from saturated solutions (5.8 M) containing 2.5×10^{-4} M commercial **1** mixture without further purification. Large (1 cm^3) blue cubes were deposited, as illustrated previously (for a photograph of such a crystal, see ref 8). There is a dye coloring threshold (2×10^{-4} M). The absorbance of the dissolved crystals varied between 558 and 545 nm, depending upon the depth of staining. For a typical batch of crystals containing 2.5×10^{-4} M **1**, there were 5.5×10^4 moles of $NaClO_3$ for every mole of **1**, as determined from the known weight of dissolved mixed crystals using the experimentally determined extinction coefficient of the commercial sample.

In order to analyze the dye inside the crystals of $NaClO_3$, we turned to MALDI-TOF MS in the negative-ion mode. Ground, dissolved crystals were treated with typical crystalline MALDI hosts such as cyano-4-hydrocinnamic acid or 2,5-dihydroxybenzoic acid. Ions were observed at *m*/*z* 776, corresponding to trisulfonated **1** associated with one Na^+ ion. Also detected was a peak at *m*/*z* 856 indicating some tetrasulfonated **1**. We conclude that these triarylmethane dyes are the major constituents in dyed $NaClO_3$. Disulfonates in the purple component were not overgrown by $NaClO_3$.

{001} Sections. The maximum and minimum absorbances of {001} plates excised with a wire saw (see the Experimental Section) were determined in polarized light using a homemade microabsorption spectrophotometer with mechanically modulated linear polarization states. The maximum absorbance for a (001) plate varied between 542 and 550 nm, depending upon the direction of incident polarization. The maximum absorbance of Perucca's $NaClO_3$ mixed crystals was 545 nm.[6]

The plates were not homogeneous. While large crystals appeared to be homogeneously colored, sections showed parallel deposition bands of greater and lesser optical density representing regions of changing dye incorporation rates, even at constant temperature. This is likely related to the changing microtopography of the growth faces.

The varying optical density represents a random inhomogeneity. However, there exists a systematic inhomogeneity of (001) sections. The plates contain five areas (or tiles) that represent cross sections of the (100), ($\bar{1}$00), (010), (0$\bar{1}$0), and (001) growth sectors (Figure 1b). Only the pairs (100)/($\bar{1}$00) and (010)/(0$\bar{1}$0)

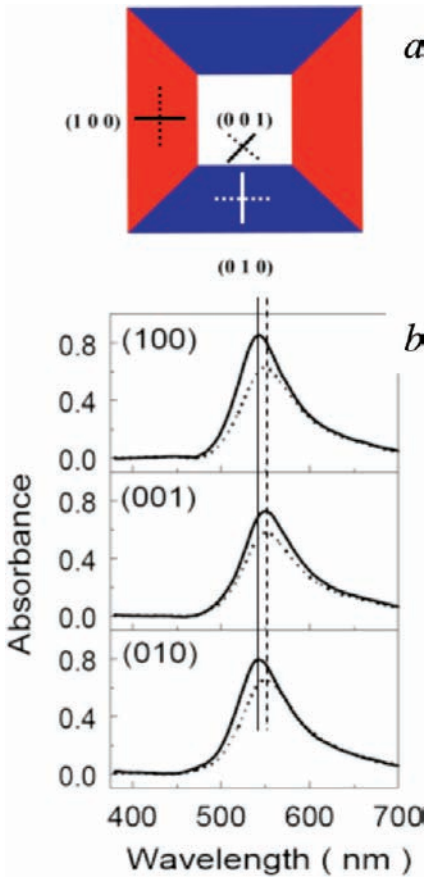

Figure 2. (a) Sketch showing a (001) plate containing five areas that represent cross sections of (100), ($\bar{1}$00), (010), (0$\bar{1}$0), and (001) growth sectors. (b) Absorption spectra for the sectors shown in (a). Solid and dotted spectra correspond to the solid and dotted polarization directions shown in (a). The absorbance viewed normal to a section depends on the family of tiles (/100/, /010/, or /001/) from which the spectra are taken. The λ_{max} value changes by ~8 nm between the orthogonal polarization states in /100/ and /010/, as indicated by the vertical guide lines.

are related by the dyad symmetry of the principal planes normal to the (001) plate face. $NaClO_3$ has T (23) symmetry in the space group $P2_13$. Thus, we expected to observe three distinct properties in the (001) sections when viewing normal to those sections. We will hereafter adopt the notation |*hkl*| to refer to a tile associated with a growth face contained within some (*hkl*) crystallographic section and use the notation /*hkl*/ to refer to any family of symmetry-related tiles in a given section.

In lateral |100| and |010| tiles of a (001) section, it is clear that λ_{max} changes by ~8 nm between orthogonal polarization states, as indicated by the guide lines in Figure 2. This change in energy with polarization is indicative of more than one electronic transition. In the central square tile that represents a cross section of the (001) growth sector, the absorption energy of **1** does not change with the linear polarization state, indicating that only one of the two electronic excitations is accessed with polarization in the plate face.

We employed the rotating polarizer technique as embodied in the Metripol microscope in order to make *images* of the linear dichroism.[33] The analysis of this type of data was described in detail previously.[7,34] The instrument produces images of tanh(ε), where $\varepsilon = 2(T_{||} - T_{\perp})/(T_{||} + T_{\perp})$, in which $T_{||}$ and $T_{\perp}$ are the transmittances for orthogonally polarized directions (Figure 3a). The corresponding map of the most strongly absorbing direction is plotted in degrees counterclockwise from the horizontal

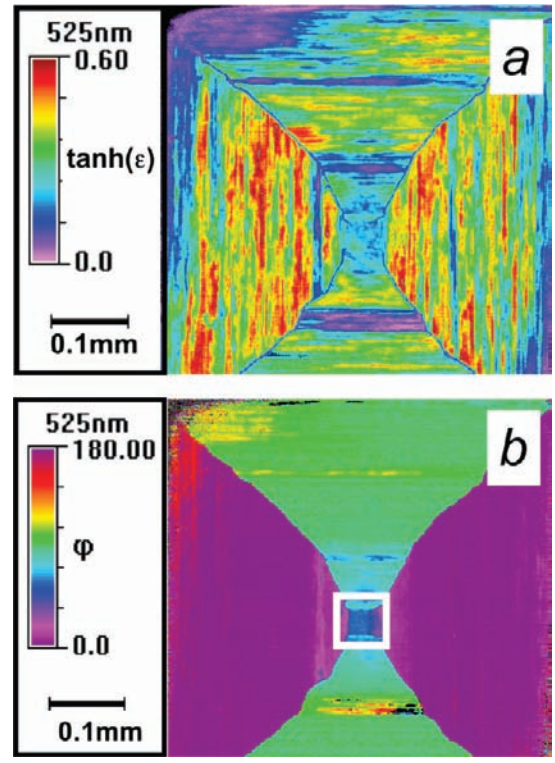

Figure 3. Images related to linear dichroism produced by the rotating polarizer technique in a (001) plate in a $NaClO_3$ crystal dyed with **1**. (a) False-color image plotted as tanh(ε), where $\varepsilon = \Delta T/T_0$, in which ΔT is the difference in transmission along orthogonal eigenmodes and T_0 is the average transmittance. (b) Corresponding map of the most strongly absorbing direction plotted in degrees counterclockwise from the horizontal for the |100|, |010|, and |001| tiles. The orientation of the oscillator in |001| reflects the red transition even when measured on the blue side of the absorption maximum because the blue transition here is orthogonal to the face and has a vanishing projection.

(Figure 3b). The magnitude of the anisotropy is greatest in the lateral sectors. The most strongly absorbing direction is perpendicular to the {100} and {010} growth faces. |001| is set off in a white box in Figure 3b. In |001|, the difference between *d*- and *l*-$NaClO_3$ is whether the optical orientation in the middle section is 45 or 135°, respectively, for sections with the group facing *up*. An obvious judgment to be drawn from these images is that the mean plane of the molecular π system is aligned in excess along the growth-face diagonals and standing on end.

The measurement of circular dichroism (CD), the differential transmittance of left and right circularly polarized light (CPL), has been described previously.[4,35] We used mechanically modulated optical components to create accurately defined polarization states in order to separate chiroptical perturbations from the obscuring effects of linear dichroism (LD) and linear

(32) Also called water blue or aniline blue, with CI no. 42755. It should be noted that the name "aniline blue" is sometimes associated with a mixture and sometimes associated with the *minor* component of the mixture, acid blue 22. Thus, there is considerable confusion as to precisely what compound Perucca used (see note 29) and precisely what compounds are at issue in spectroscopic and histochemical studies involving "aniline blue".

(33) Glazer, A. M.; Lewis, J. G.; Kaminsky, W. *Proc. R. Soc. London, Ser. A* **1996**, *452*, 2751–2765. Kaminsky, W.; Gunn, E.; Sours, R.; Kahr, B. *J. Microsc.* **2007**, *228*, 153–164.
(34) Benedict, J. B.; Cohen, D.; Lovell, S.; Rohl, A.; Kahr, B. *J. Am. Chem. Soc.* **2006**, *128*, 5548–5549.
(35) Claborn, K.; Puklin-Faucher, E.; Kurimoto, M.; Kaminsky, W.; Kahr, B. *J. Am. Chem. Soc.* **2003**, *125*, 14825–14831.

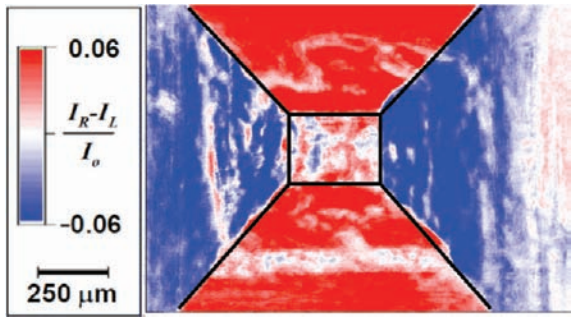

Figure 4. Circular dichroism of the (001) plate shows opposite signs for the |100| and |010| tiles and a comparatively small value for |001|.

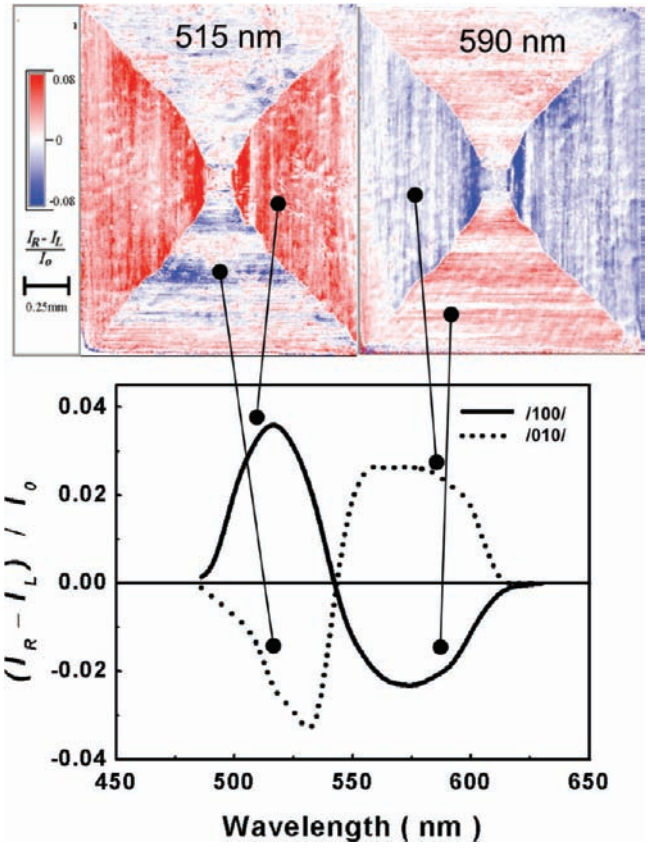

Figure 5. (bottom) Circular dichroism plotted as function of wavelength and (top) corresponding CD micrographs taken at 515 and 590 nm showing the change in the sign of the effect upon moving from the blue side to the red side of the absorption maximum.

birefringence (LB). The circular transmission differences were as large as 5% and were 3% when averaged over 0.1 mm^2 areas. Curiously, the sign of the differences for /100/ and /010/ were opposite (Figure 4). The CD in |001| was negligible. The sign of the effect changed not only from tile to tile but also within a tile upon moving from the blue side to the red side of the absorption maximum, as shown in Figure 5. The line shapes for both |100| and |010| are bisignate. However, while the pair of curves resemble the responses of enantiomers, the absence of true mirror image line shapes is highly reproducible. There are no enantiomorphous chiroptical effects to be expected in a single $NaClO_3$ crystal with a given handedness in the space group $P2_13$.

Crystals grown at room temperature gave a barely discernible CD signal [$(I_R - I_L)/I_0 \approx \pm 0.01$]. This difference prompted us

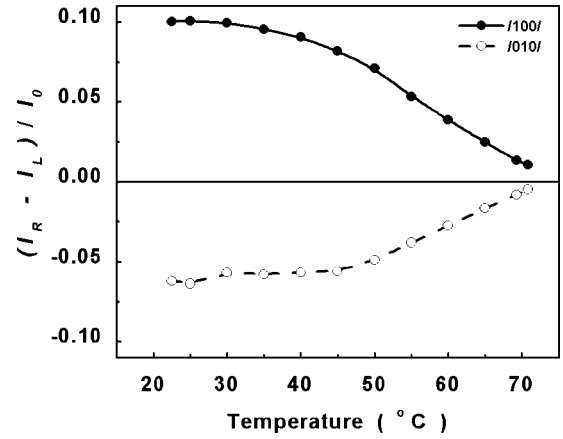

Figure 6. Declination in the CD signal at 490 nm for the |100| and |010| tiles in a (001) $NaClO_3$ plate dyed with **1**. The temperature was raised in 5° increments and held at each temperature for 10 min.

to investigate the effect of temperature on the optical properties of crystals grown at 5 °C. Indeed, at ~45 °C, the CD and LD began to decline. The diminution of the CD signal with temperature is shown in Figure 6. With each increase in temperature, we observed a small decrease in signal intensity that ultimately reached a plateau with time. Only upon a further increase in temperature could we drive the dichroic responses to very small values. This is consistent with dynamic processes having dispersive kinetics, a common expectation for reactions within crystals. To assay the activation energy associated with the decline of the CD, the signal decay at 490 nm was plotted as a function of time for crystals brought rapidly to 47, 52, 57, 62, 67, and 72 °C. There was an initial precipitous decline, which when treated as a first-order Arrhenius process gave an activation energy of 136 ± 15 kJ/mol, followed by a more gradual loss of CD signal intensity. This energy is more than twice as high as that for the enantiomerization of a triarylmethyl carbocation in solution, a sensible value for **1** trapped in a crystal.[36] In order to prepare samples in which to study the temperature dependence of the signal, we had to polish the crystals on ground glass cooled with dry ice, as frictional heating caused a diminution in the initial value of the CD.

{110} Sections. {110} sections of cubes with *T* symmetry are asymmetric (as opposed to {001} sectors, which have dyad symmetry) and are composed of four growth sectors not related in the normal direction by symmetry (Figures 1 and 7). Because crystals spontaneously nucleated on the bottom of dishes and grew upward, only three sectors are evident in subsequent micrographs (Figures 8 and 9). Indeed, the measured spectra as well as the images related to LD were distinct for each of the symmetry-independent tiles (Figures 7−9). All of the spectra in Figure 7 show an energy shift indicating that some component of the transition electric dipole moment in each of the red and blue transitions is projected onto the sample plane. The images related to LB and LD are shown in Figure 8.

The {110} section gave strong circular extinction (CE) signals: −0.035, −0.004, and +0.04. Extinction, the sum of absorption, light scattering, and any other mechanism that would attenuate left or right CPL, is a more general term than absorption. We hesitate to call the aforementioned contrast a consequence of CD for reasons that will be explored at length

(36) Schuster, I. I.; Colter, A. K.; Kurland, R. J. *J. Am. Chem. Soc.* **1968**, *90*, 4679–4687.

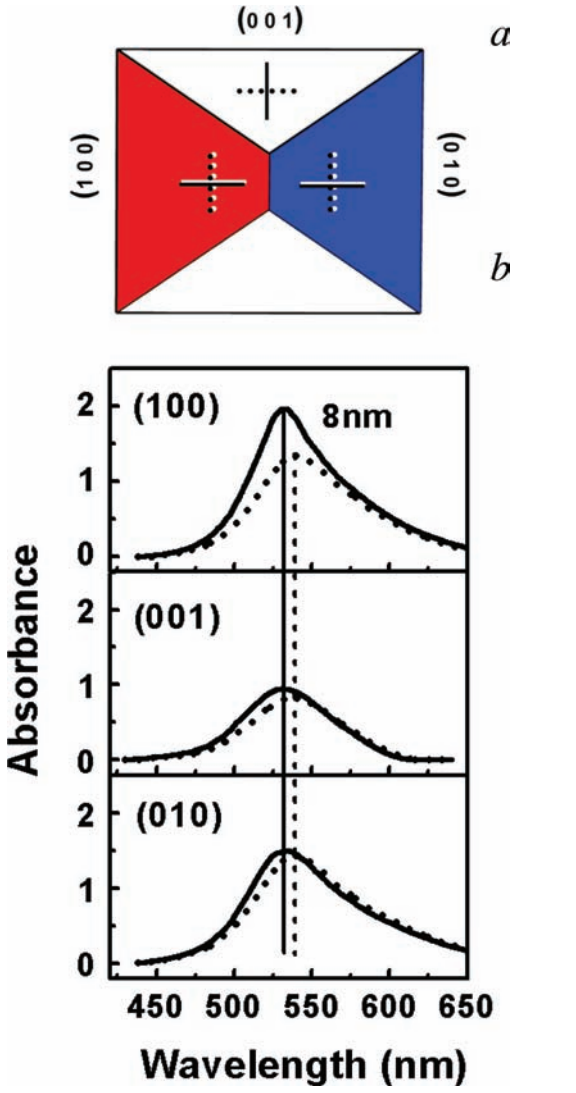

Figure 7. (a) Schematic (110) section showing /100/, /001/, and /010/ tiles of cubes not related by symmetry in this plane. (b) Absorbance viewed normal to the /100/, /001/, and /010/ tiles in (110) sections; λ_{max} changes of ~8 nm between orthogonal polarization states are indicated by the guide lines. The coloring in the crystal drawing is keyed to the micrographs in Figure 9.

in the Discussion. Unlike the {100} sections, the CE curves for the left and right sectors of the {110} sections are monosignate; they resemble the absorption band in Figure 7. The {110} sections are further differentiated from the {100} sections in their transformation properties. When {100} plates are turned over on the microscope, in effect changing the sign of the wave vector, the sign of the CE is invariant. However, {110} plates have antisymmetric CE with respect to the sign of the wave vector. This distinction clearly indicates that we are observing distinct optical phenomena in the {100} and {110} sections. The nature of this difference will be discussed below.

{111} Sections. The {111} sections provide an important control. Because adjacent {111} sectors are related by the threefold body-diagonal rotations, which are genuine symmetry operations in the point group *T* (23), these sectors should manifest the same optical properties. For this reason, the /100/ tiles in the {111} sections are similarly shaded in Figure 1. Indeed, the polarization spectra, LD images, and CE images are the same for all three tiles [|100|, |010|, and |001|] of a (111) slice. The transformation properties of the CE signal more

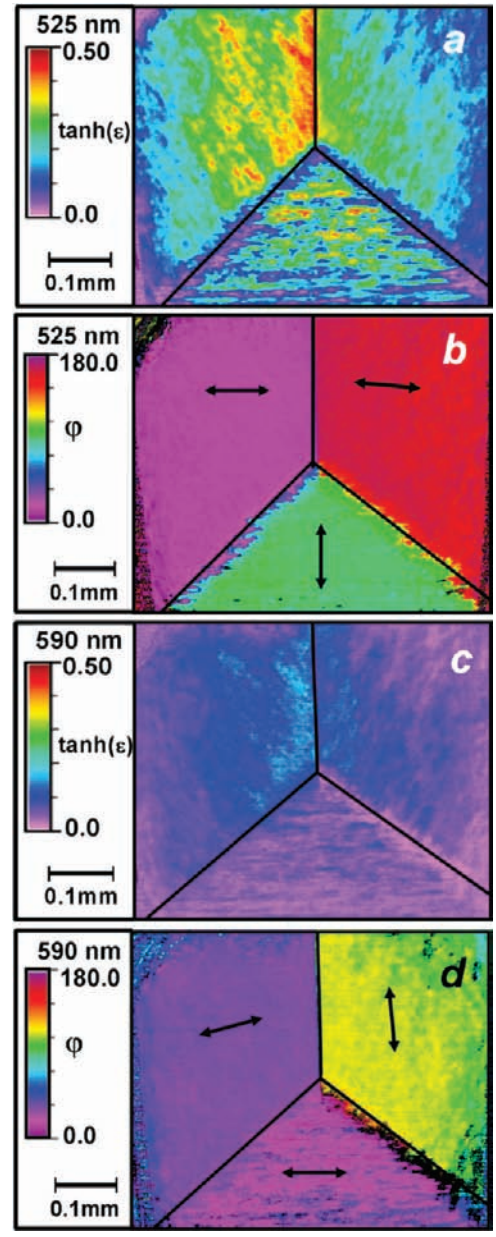

Figure 8. Distinct linear dichroism images for each of the symmetry-independent tiles in the (110) plate. (a, c) False-color images related to the linear dichroism [measured at tanh(ε), where $\varepsilon = \Delta T/T_0$]. (b, d) Corresponding maps of the most strongly absorbing direction φ (double arrows) plotted in degrees, taken at the blue side of the absorption maximum (525 nm) and the red side of the absorption maximum (590 nm), respectively. The tiles are delineated by the thin black lines.

closely resembled those of the {110} sections. The effect was antisymmetric with respect to the wave vector. The difference between the {111} and $\{\bar{1}\bar{1}\bar{1}\}$ plates is whether the dipoles are radial or tangential. For *d*-$NaClO_3$, the sections with radial dipoles were established as {111} by the method of the anomalous dispersion of X-rays.

Computations

We computed[37] the rotatory strength tensors $\mathbf{R}_{\pi^*-\pi}$ for the lowest-energy $\pi \rightarrow \pi^*$ transitions of **3** [in which the three sulfonate groups of **1** were replaced with hydrogen atoms

(37) Autschbach, J. *Chirality* **2009**, *21*, E116–E152.

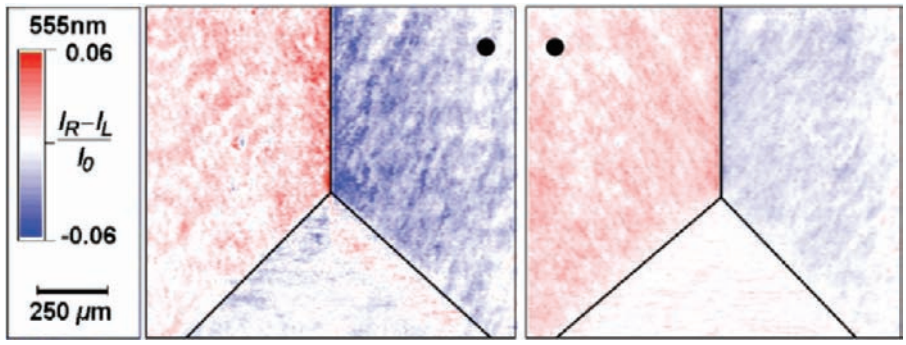

Figure 9. Circular extinction (CE) signals at 555 nm for the (110) plate, showing the change in the sign of the signal when the plate is rotated about the vertical axis. The /100/, /010/, and /001/ tiles are delineated by the thin black lines. The black dots indicate the same area before and after the plate was turned over.

Table 1. Calculated Spectroscopic Parameters

			symmetric rotatory strength tensors **R** (unique values only) (10^{-40} esu^2 cm^2)							
			components							
compound [total energy (eV)]	transition energy (eV)	oscillator strength	*xx*	*xy*	*yy*	*xz*	*yz*	*zz*	eigenvalues	dissymmetry factor $4R/D$[a]
$\mathbf{3_S}$ [−1592.375]	2.342	0.853	342.68	244.65	−333.81	−305.43	1356.56	−193.25	−1698, 413, 1099	−0.0071
	2.346	0.843	−343.60	−244.81	350.35	288.42	−1366.02	−206.02	1540, 412, −1327	0.0065
$\mathbf{3_A}$ [−1592.373]	2.345	0.950	98.12	−134.62	−204.27	−604.51	−1198.12	−304.04	−1620, 145, 1066	−0.0060
	2.348	0.724	245.86	180.80	−54.24	−159.00	1791.36	112.83	1823, 274, −1792	0.0089

[a] Based on the largest absolute eigenvalue.

(Scheme 1)] using time-dependent density functional theory with the B3LYP functional[39] and the 6-311G** basis set, as embodied in Gaussian 09.[38] Sulfonate groups typically are electronically inert. The removal of the sulfonates decreased the computational time and facilitated convergence, liberating us from having to devise a model to compensate for the effects of the three negative charges. Two equi-energetic conformations, designated as $\mathbf{3_S}$ (symmetric, point group C_3) and $\mathbf{3_A}$(asymmetric, point group C_1), were analyzed. The total energies, electronic excitation energies, and oscillator strengths as well as the rotatory strength tensor components, eigenvalues, and dissymmetry factors are listed in Table 1.

The magnitude surfaces of the computed tensors (Figure 10) were plotted with respect to spherical polar angles (θ, ϕ) as $R_{\pi^*-\pi}(\theta, \phi) = \mathbf{u}^T(\theta, \phi)\mathbf{R}_{\pi^*-\pi}\mathbf{u}(\theta, \phi)$, where $\mathbf{u}$ is a propagation vector.[40] The surface maxima share directions in a plane perpendicular to the mean molecular planes. For both the red and blue transitions of $\mathbf{3_S}$ and $\mathbf{3_A}$, the representation surfaces contained significant positive and negative maxima in orthogonal directions. In all cases, a much smaller value of the tensor in the mean molecular plane was obtained. $\mathbf{3_A}$ is more consistent with experiment because the tensors more closely approximate the diagonal form [0 0 0; 0 x 0; 0 0 $-x$] having equally large positive and negative values with a null in the orthogonal direction.

Discussion

X-ray and Electronic Structures of Triarylmethyl Cations. Any interpretation of the chiroptical properties of **1** (or any molecule, for that matter) rests on an understanding of electronic structure. The most well studied congener of **1** is the per-N-methylated compound crystal violet (**4**). We previously determined the crystal structures of two hydrates of **4** chloride, a monohydrate[41] and a nonahydrate.[42] The average dihedral angles between the aryl rings and the plane of coordination of the central carbon atoms are 33 and 28°, respectively.[43] In the monohydrate, the molecules sit on general positions, whereas in the nonahydrate, the molecules sit on special positions and have the symmetry of trigonal propellers. Comparable twists (32°) were observed in **1** and the unsubstituted triphenylmethyl cation (**5**).[44,45] It has been well-established that degenerate or nearly degenerate $\pi \rightarrow \pi^*$ transitions determine the interactions of symmetrically substituted triarylmethyl propellers with visible light.[46]

Molecular orbital calculations on symmetric triarylmethyl propellers are consistent with a degenerate pair of (x, y)-polarized transitions from the A_1 ground electronic state to an excited E state. The degeneracy can be lifted through unsymmetrical substitution of the three aryl rings or by conformational distortion of the triarylmethyl propellor from its ideal D_3-symmetric ground state, usually along the two ring-flip isomerization pathway to a C_2 conformation.[42] Conformational differences among the para substituents may likewise cause a

(38) Frisch, M. J.; et al. *Gaussian 09*, revision A.02; Gaussian, Inc: Wallingford, CT, 2009.
(39) Becke, A. D. *J. Chem. Phys.* **1993**, *98*, 5648–5652. Stephens, P. J.; Devlin, F. J.; Chabalowski, C. F.; Frisch, M. J. *J. Phys. Chem.* **1994**, *98*, 11623–11627.
(40) Hansen, A. E.; Bak, K. L. *J. Phys. Chem. A* **2000**, *104*, 11362–11370.
(41) Kahr, B.; Kelley, M. P. In *Supramolecular Stereochemistry*; Siegel, J. S., Ed.; Kluwer Academic Publishers: Dordrecht, The Netherlands, 1995; pp 203−221.
(42) Lovell, S.; Marquardt, B. J.; Kahr, B. *J. Chem. Soc., Perkin Trans. 2* **1999**, *2*, 2241–2247.
(43) Also see: Spangler, B. D.; Vanysek, P.; Hernandez, I. C.; Rogers, R. D. *J. Cryst. Spectrosc. Res.* **1989**, *19*, 589–596.
(44) Gomes de Mesquita, A. H.; MacGillavry, C. H.; Eriks, K. *Acta Crystallogr.* **1965**, *18*, 437–443.
(45) Koh, L. L.; Eriks, K. *Acta Crystallogr.* **1971**, *B27*, 1405–1413.
(46) Duxbury, D. F. *Chem. Rev.* **1993**, *93*, 381–433.

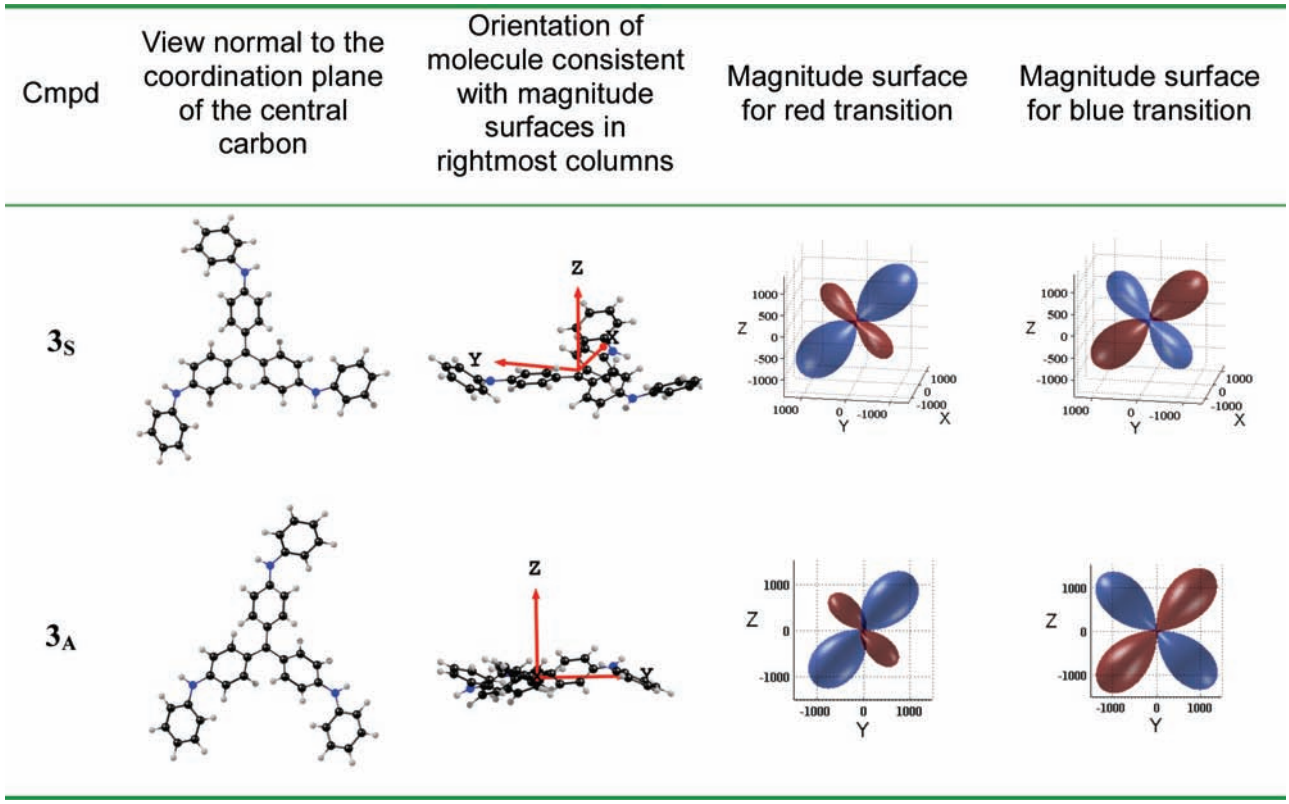

Figure 10. Calculated circular dichroism magnitude surfaces (10^{-40} esu^2 cm^2) for the nominally degenerate excitations of $\mathbf{3_S}$ and $\mathbf{3_A}$. For the actual dimensions, see Table 1.

desymmetrization (as in $\mathbf{1_A}$ and $\mathbf{3_A}$) without significantly distorting the propeller-shaped core.

Determination of the Circular Dichroism Tensor of an Anisotropic Crystal. Four independent measurements are required to fix the CD tensor of $NaClO_3$/**1** mixed crystals. (001) plates present molecules of **1** along three independent Cartesian directions corresponding to the three symmetry-independent tiles. A fourth measurement is provided by the (110) section. In both the central |001| tile of the (110) section and the |001| tile of a (100) section, the CD vanishes. This defines the null planes of the CD tensor as ⟨110⟩. In the /010/ and /100/ tiles of a (001) section, the CD values are nearly equal in magnitude and opposite in sign, consistent with equal-magnitude but oppositely signed CD with maximal absolute values along *a* and *b* (see Figures 4 and 9). Thus, we can orient the CD tensor with respect to the growth faces as in Figure 11. From one growth face to adjacent growth faces, the tensor is rotated by $\pm 2\pi/3$ about the body diagonals.

Correspondence Between Calculations and Experiment. The form of the calculated rotatory strength tensor for $\mathbf{3_A}$ and the CD response for **1** in $NaClO_3$ are in qualitative accord on the basis of an examination of Figures 4, 10, and 11; both theory and experiment point to bisignate CD tensors with substantial + and − character in orthogonal directions that change sign between the degenerate or near-degenerate $\pi \rightarrow \pi^*$ transitions. Is there also quantitative agreement between the experimental quantity $(I_R - I_L)/I_0$ (expressed as a fraction of 1) and the computed rotatory strength in the system of atomic units? The correspondence was established in the following way: Typical values of the quantity $(I_R - I_L)/I_0$ were ∼0.03. We can say that $(I_R - I_L)/I_0 = [e^{-A+(\Delta A/2)} - e^{-A-(\Delta A/2)}]$, where A is the average absorbance of the crystals and ΔA is the difference in the absorbances of left and right CPL. The average absorbance for the crystals we studied was ∼0.8 (Figure 2). Thus, ΔA must equal 0.08 to give $(I_R - I_L)/I_0 \approx 0.03$. We can further state that $\Delta A/A$ is equal to $4R/D$, where R is the rotatory strength and D is the dipole strength.[47] Converting the unitless oscillator strength to dipole strength D (in cgs units) requires dividing by the factor $(8\pi^2 \nu m_e c)/(3he^2)$, where ν is the frequency of the transition in cm^{-1}, m_e is the mass of the electron, c is the speed of light, h is Planck's constant, and e is the electron charge. Converting the rotatory strength R from atomic to cgs units

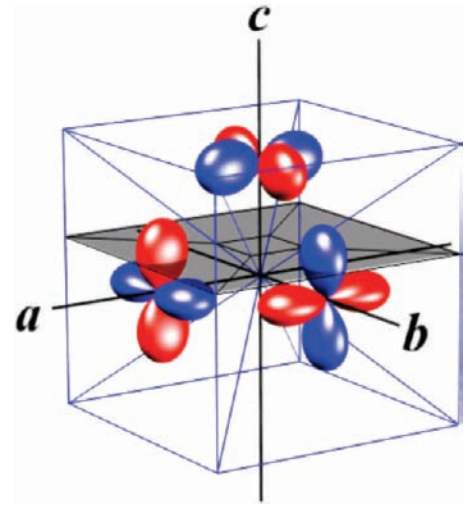

Figure 11. Arrangement of an idealized, equivalued bisignate representation surface of the circular dichroism tensors in the (100), (010), and (001) growth sectors, which are related to one another by rotation about [111], the threefold body diagonals in the space group $P2_13$.

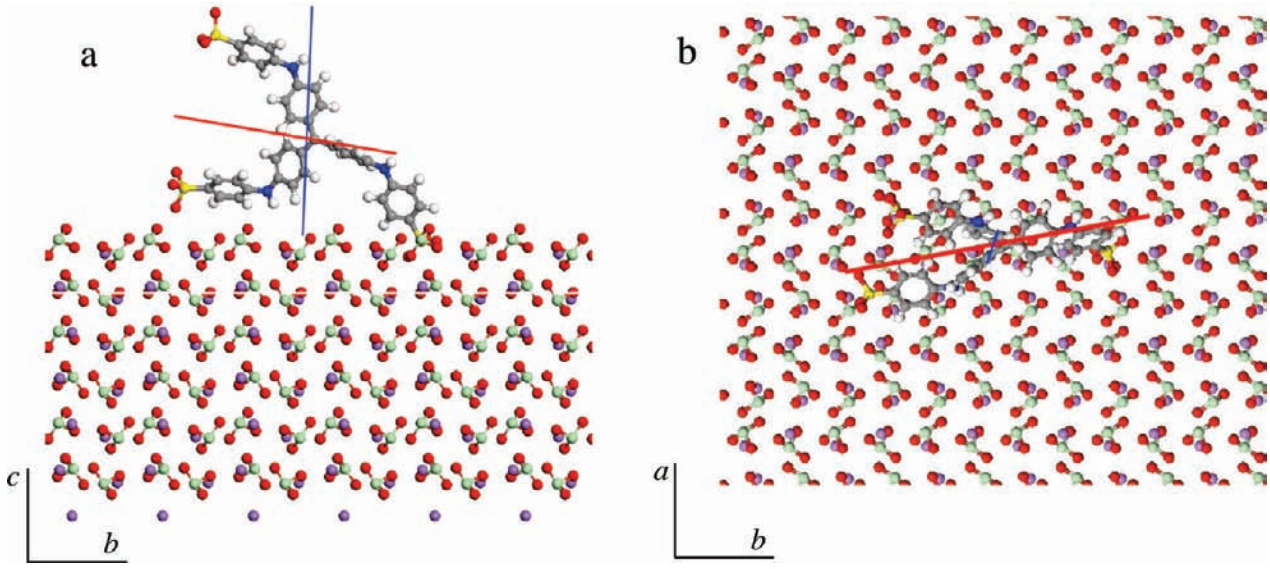

Figure 12. Arrangement of $\mathbf{1_A}$ on the (001) surface of *d*-$NaClO_3$, with lines representing the blue and red transition moments. (a) View along [100]. Sulfonates were substituted at the para positions of $\mathbf{3_A}$, and this structure was placed on the surface with one of the sulfonate groups replacing a chlorate group. The blue transition thus ends up in the near-normal position. The conformation of the side chains was then optimized using the universal force field in the Materials Studio modeling suite with little change in the effective model. (b) View along [001]. The modest dichroic ratio in Figure 3 predicts some averaging (presumably there is more than a single orientation) not embodied in (b).

requires multiplication by the factor $(e^2ha_0)/(2\pi m_e c)$, where a_0 is the Bohr radius.[48] From the computed values for $\mathbf{3_A}$ in Table 1, D is $\sim 5 \times 10^{-35}$ esu^2 cm^2; $4R$ is therefore $\sim 3 \times 10^{-37}$ esu^2 cm^2. The quantity $4R/D$ equals 0.007 on average for the compounds modeled in Table 1 and Figure 10. $\Delta A/A \approx 0.1$. The computed expectation is thus $\sim$14 times smaller than the experimental data. Some measure of the experimental signal (but less than half because of the transformation of signs upon inversion of the sign of the wave vector) can be attributed to ACE as opposed to natural CD. In this way, the computed expectation is $\sim$10 times smaller than experiment.

Does a discrepancy of 1 order of magnitude indicate good or poor agreement with experiment? Since the computed values are based upon idealized, gas-phase geometries while the experimental data come from chromophores buried within an optically complex ionic crystal, precise agreement (had we achieved it) would have to be judged fortuitous. As there are not any comparable studies that establish a context for the present analysis, it is difficult to judge whether the measurements or the computations are further from the mark. Indeed, they might both be very accurate, with their difference arising from the crystal perturbations of the chiroptical properties. It is well-known that basis sets, vibrational corrections, and solvation can have large effects on computed chiroptical properties.[49] Likewise, solvation plays an enormous role in determining the average values of experimental optical rotation and CD[50] in solution. Agreement between theory and experiment is seen in the broadest features: the changes in sign with orientation and wavelength.

Because $\mathbf{1_A}$ has a computed tensor nearer to experiment, with two large, oppositely signed values and a null or near-null in the mutually orthogonal direction, we considered how its sulfonate analogue, $\mathbf{3_A}$, might sit on the (100) face of $NaClO_3$. On the crystal surface, the orientation of a pair of symmetry-related chlorates can be expressed as a vector defined by the centroid of the three oxygen atoms and the chlorine atom position. This vector makes an angle of 35° with the surface normal. We substituted $-SO_3^-$ groups for the hydrogens in $\mathbf{3_A}$ to create a model for $\mathbf{1_A}$. We best superimposed one *p*-SO_3^- for a pyramidal ClO_3^- on the surface. A great deal of evidence supports the superposition of sulfonates for oxy anions in the analysis of mixed crystal structures.[51] The blue transition electric dipole moment in this configuration makes an angle of 7° to the surface normal. Experiments were unable to detect any component of this transition in the {100} planes, predicting an angle of $0° \pm 5°$. When the structure was allowed to relax under the constraints of a fixed crystalline monolith and the universal force field in the Materials Studio software suite, the blue transition stayed upright, making an angle of 14° with the surface normal (see the model in Figure 12a). It has not escaped our notice that the two sulfonates not located on the surface correlate well with the position of chlorate ions in the step that would approach from the left in Figure 12a. Figure 12b shows the inclination of the red dipole. The interpretation of this angle is limited by the mutual interaction of LD and a weak but nonzero LB.

Circular Dichroism versus Anomalous Circular Extinction. Generally, an object must lack a center of symmetry to be sensitive to the handedness of light. In the case of ACE-active materials, the anisotropy of the host can contribute a linear component to the polarization state of the light, producing orthogonal elliptically polarized states for right circularly polarized (RCP) and left circularly polarized (LCP) input states.

(47) Nafie, L. A.; Freedman, T. B. In *Circular Dichroism: Principles and Applications*, 2nd ed; Berova, N., Nakanishi, K., Woody, R. W., Eds.; Wiley-VCH: Weinheim, Germany, 2000; p 100.
(48) Kongsted, J.; Pedersen, T. B.; Osted, A.; Hansen, A. E.; Mikkelsen, K. V. *J. Phys. Chem. A* **2004**, *108*, 3632–3641.
(49) Crawford, D. *Theor. Chem. Acc.* **2006**, *115*, 227–245.
(50) Muller, T.; Wiberg, K. B.; Vaccaro, P. H. *J. Phys. Chem. A* **2000**, *104*, 5959–5968.
(51) Carter, D. J.; Rohl, A. L.; Gale, J. D.; Fogg, A. M.; Gurney, R. W.; Kahr, B. *J. Mol. Struct.* **2003**, *647*, 65–73. Carter, D. J.; Ogden, M. I.; Rohl, A. L. *J. Phys. Chem. C* **2007**, *111*, 9283–9289. Bastin, L. D.; Kahr, B. *Tetrahedron* **2000**, *56*, 6633–6643. Kelley, M. P.; Janssens, B.; Kahr, B.; Vetter, W. M. *J. Am. Chem. Soc.* **1994**, *116*, 5519–5520.

The interactions of a rodlike absorbing dipole with the two elliptical light forms need not be the same as long as the transition moment of the dye does not align with an eigenmode of the medium about which the dyes will be counter-rotated for RCP and LCP light. This overly simple model treats the crystal as consisting of two layers, one contributing a phase shift δ and the other a dipole interaction. The birefringence of the medium creates a phase shift of $\sim\pi/2$ (one-quarter of a wavelength), converting LCP light into linearly polarized light (the extreme ellipticity) at $+45°$ and RCP into linearly polarized light at $-45°$ with respect to the fast axis of the host. The polarization state of the orthogonal light forms is further attenuated by interaction with the inclined dipoles by a degree sensitive to their orientation, resulting in a net differential transmission of light. It follows that a positive CE signal $(I_R - I_L)/I_0$ corresponds to an induced dipole inclined clockwise from the vertical direction. Consistent with the observed phenomenon of ACE, this model predicts that the signal should change sign when the sample is rotated by 180° around one of the eigenmode directions. This optical transformation is inconsistent with intrinsic CD and optical rotation, which are independent of the sign of the wave vector, and is therefore a telltale sign of ACE.

In order to observe the ACE effect, the crystals must manifest distinct eigenmodes. That is, the crystals must show anomalous LB.[52] They indeed do in the present work, as shown in Figure 13a,b for a (100) section. However, the transition moments are aligned with the eigenmodes in a (100) projection, a condition that obviates ACE. Indeed, in the (100) sections, we observe largely CD, as indicated by the fact that the signal is independent of the sign of the wave vector; the effect does not change sign when we flip the crystals over (see Figure 14). In (110) sections, we see a correlation between the tiles that show ACE and the tiles that have strongly defined eigenmodes (|100| and |010|). The |001| is not birefringent at 470 nm in the |001| tile, nor does it show any ACE signal (let alone a CD signal, as we are looking along the null of the CD tensor). However, as a result of the mixing of the red and blue transitions, the ACE magnitudes in these sections, and the positions of the eigenvectors, are strongly wavelength-dependent.

Resolution of Simple Triarylmethyl Propellers. The triphenylmethyl cation, radical, and anion, as well as their symmetrical congeners, are chiral propeller-shaped molecules with D_3 symmetry in their ground states. Triphenylborane and triphenylamine are isomorphous with their congeners having central carbon atoms. However, in solutions at room temperature, almost all such compounds are optically inactive equilibrium racemic mixtures. Only the perchlorotriphenylmethyl radical and the isomorphous perchlorotriphenylamine[53] have been resolved. This is a consequence of the six bulky *o*-chloro substituents that decrease the rates of racemization by the two-ring flip threshold mechanism, enabling chromatographic separation on a chiral stationary phase. The chiroptical responses of such compounds tend to be very large. For instance, the specific rotation ($[\alpha]^{25}_{435}$) of (+)-perchlorotriphenylamine is 2385°.[54]

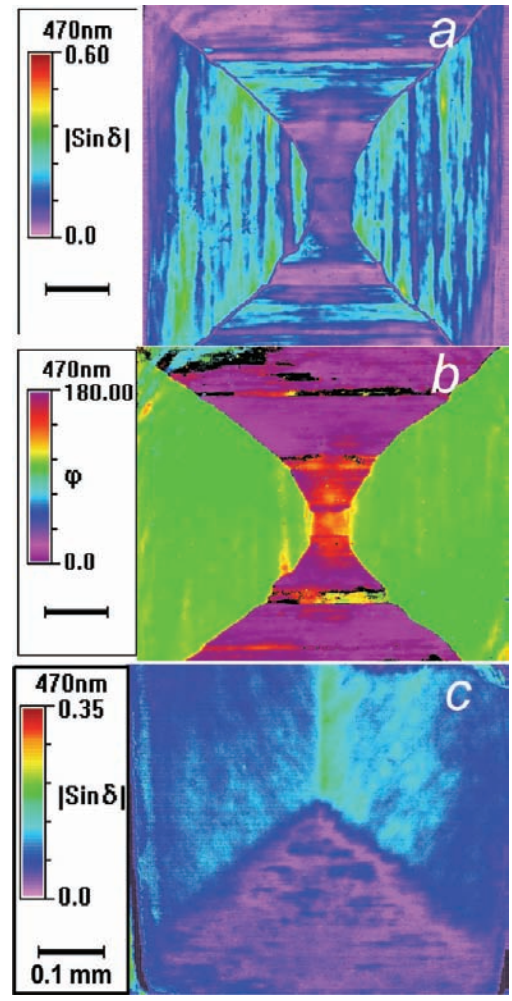

Figure 13. Off-resonance (470 nm) micrographs of images related to linear birefringence ($\delta = 2\pi\Delta nL/\lambda$, where Δn is the linear birefringence) for (a, b) (100) and (c) (110). Panels (a) and (c) are represented as |sin δ|, and panel (b) shows the direction of the largest refractive index, measured as φ in degrees counterclockwise from the horizon.

No triarylmethyl propellers lacking bulky ortho substituents have been resolved. By virtue of our large chiroptical signature in $NaClO_3$/**1**, it appears that we have indeed accomplished such a resolution.

Our chiroptical intuition is developed from solution studies. In solutions, if we begin with a racemic mixture and develop a chiroptical signal, we have accomplished a chemical resolution. This is not so in crystals. Our analysis of the bisignate CD tensors of $\mathbf{3_S}$, $\mathbf{3_A}$, and **1**-stained $NaClO_3$ reveal that in the absence of an unequivocal association mechanism of crystal and dye, it is impossible—because of the bisignate character—to assign the sense of the propeller-shaped molecules that are associated with the crystals. When a chiroptical signal is bisignate and dependent upon orientation, it is surely possible to have *P* and *M* enantiomers in different (or mirrorlike) orientations within $NaClO_3$, which means that their tensors are additive. In other words, it is possible to have within any one crystal equal populations of oppositely handed propellers (we are careful here not to say a "racemate", as we cannot have enantiomers within a chiral host) without any diminution in the CD. Such a situation is illustrated in Figure 15. Symmetry certainly permits such a scenario.

(52) Kahr, B.; McBride, J. M. *Angew. Chem., Int. Ed. Engl.* **1992**, *31*, 1–26. Shtukenberg, A.; Punin, Y. O. *Optically Anomalous Crystals*; Kahr, B., Ed.; Springer: Dordrecht, The Netherlands, 2007.

(53) Irurre, J.; Santamaria, J.; Gonzalezrego, M. C. *Chirality* **1995**, *7*, 154–157. Hayes, K. S.; Nagumo, M.; Blount, J. F.; Mislow, K. *J. Am. Chem. Soc.* **1980**, *102*, 2773–2776.

(54) Okamoto, Y.; Yashima, E.; Hatada, K.; Mislow, K. *J. Org. Chem.* **1984**, *49*, 557–558.

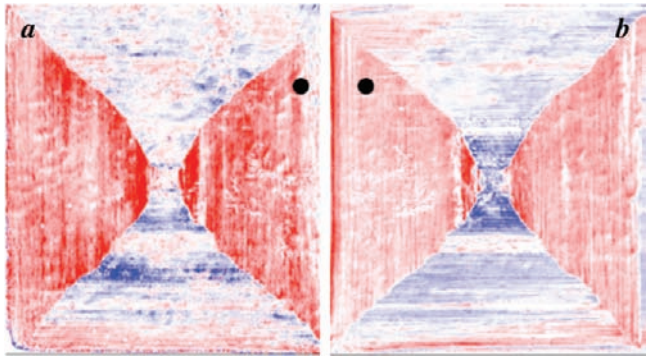

Figure 14. CD micrographs of the (100) section. The black dots indicate the same area before and after the plate was flipped around the vertical axis from side *a* to side *b*.

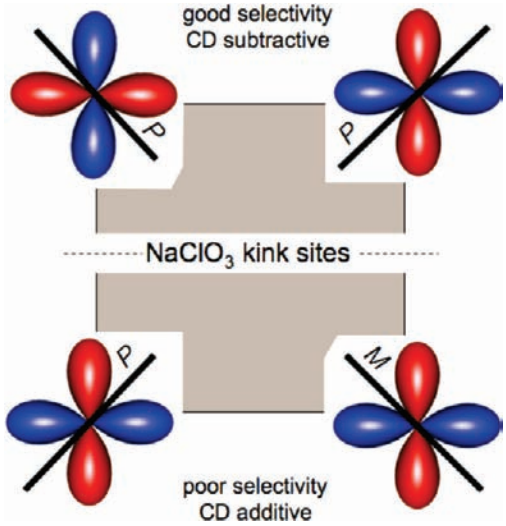

Figure 15. (top) Propellers of like handedness (*P*) having idealized bisignate rotatory responses that cancel one another because the propellers adopt distinct orientations in the asymmetric lattice. (bottom) Enantiomers recognizing distinct kink sites but having orientations leading to an additive contribution of their rotatory power. The kinks are shaped only to express the dyad symmetry of the principal faces. Diagonal black lines indicate the mean planes of the π systems.

However, because a single $NaClO_3$ crystal is chiral, one can argue on the basis of symmetry alone that the populations of *P* and *M* enantiomers cannot be precisely equal, nor can their conformations be precisely the same. In addition, the decrease in the CD signature upon sample heating proves enantioselection *at given sites* during crystal growth. There is no question that we have affected a resolution, but it may not be meaningful from the perspective of, say, the pharmaceutical sciences. Similarly, it is possible to have a complete resolution of *P* and *M* propellers but in two orientations that result in cancellation of the CD. These conclusions are wholly different than the expectations based upon measurements of CD in solution.

Conclusion: What Perucca Observed

Analysis of the primary data in Perucca's 1919 paper revealed two troublesome facts: (1) the ORD line shape through the dye absorption band resembled the absorption envelope, not the first derivative of the absorption line shape, and (2) the sign and magnitude of the optical activity in his crystal depended upon the input orientation of the linearly polarized light. The line shape might be unusual as a consequence of overlapping electronic transitions. However, in light of our earlier analyses of ACE,[4,55] a phenomenon that we showed was proportional to the absorption line shape function, and on the basis of our observations of ACE in some directions in our best effort to reproduce Perucca's crystal, it is likely that the Italian pioneer was likewise observing a convolution of circular dichroism and the dispersive partner of ACE, anomalous azimuthal rotation (AAR),[4] which is likewise a consequence of absorption. Previously, we showed that AAR depends on the orientation of the input linear polarization, providing further evidence that Perucca was not measuring purely chiroptical effects. However, because CD is strong in **1**-stained $NaClO_3$, it is probable that Perucca had captured anomalous ORD in part.

What did Perucca then really achieve, and did he know what it was? Perucca did not know (nor could he be expected to know, given the development of conformational analysis in 1919) that triarylmethyl cation solutions would be equilibrium racemic mixtures of propeller-shaped molecules. Not until 1942 did Lewis first suggest that triarylmethyl cation rings cannot be mutually planar because of steric hindrance.[56,57] Seel independently proposed the triphenylmethyl propeller.[58] Evidence for the mutual nonplanarity of the aryl rings of triarylmethyl cations first came from IR spectroscopy[59] and was later quantified by X-ray analysis.[44]

Perucca, operating under the assumption that triarylmethanes are achiral, aspired to induce in them a chiroptical response through their noncovalent association within a chiral medium. In this he succeeded. The study of induced optical activity began 50 years later with the ORD curves of Blout and Stryer showing Cotton effects from achiral acridine dyes associated with polypeptides.[60] With the advent of electro-optic polarization modulation and the production of commercial CD spectropolarimeters, measurements of induced ORD were supplanted by CD spectra.[61]

In view of the equivocal aspects of the appearance of Perucca's paper in a world struggling to regain its own equilibrium in 1919, it is perhaps not surprising that this work went unnoticed. Fortunately, dyed crystals preserve ample optical evidence of their host−guest interactions during growth.[62] It is from just this sort of crystal that we can begin to understand the interactions of organic compounds on catalytic $NaClO_3$ crystals,[27] among others.[63] Perucca's overlooked paper may also concern researchers who study the "spontaneous

(55) Kaminsky, W.; Geday, M. A.; Herreros-Cedres, J.; Kahr, B. *J. Phys. Chem. A* **2003**, *107*, 2800–2807.
(56) Lewis, G. N.; Magel, T. T.; Lipkin, D. *J. Am. Chem. Soc.* **1942**, *64*, 1774–1782.
(57) Brunings, K. J.; Corwin, A. H. *J. Am. Chem. Soc.* **1944**, *66*, 337–342.
(58) Seel, F. *Naturwissenschaften* **1943**, *31*, 504–505.
(59) Sharp, D. W. A.; Sheppard, N. *J. Chem. Soc.* **1957**, 674–682.
(60) Blout, E. R.; Stryer, L. *Proc. Natl. Acad. Sci. U.S.A.* **1959**, *45*, 1591–1593.
(61) For reviews of induced optical activity, see: (a) Bosnich, B. In *Fundamental Aspects and Recent Developments in Optical Rotatory Dispersion and Circular Dichroism*; Ciardeli, F., Salvadori, P., Eds.; Heyden: London, 1973; pp 254−265. (b) Hatano, M., *Induced Circular Dichroism in Biopolymer−Dye Systems*; Okamura, S., Ed.; Advances in Polymer Science, Vol. 77; Springer-Verlag: Berlin, 1986. (c) Allenmark, S. *Chirality* **2003**, *15*, 409–422.
(62) Barbon, A.; Bellinazzi, M.; Benedict, J. B.; Brustolon, M.; Fleming, S. D.; Jang, S.-H.; Kahr, B.; Rohl, A. L. *Angew. Chem., Int. Ed.* **2004**, *43*, 5328–5331.
(63) Gellman, A. J.; Horvath, J. D.; Buelow, M. T. *J. Mol. Catal. A: Chem.* **2001**, *167*, 3–11. Horvath, J. D.; Gellman, A. J. *Top. Catal.* **2003**, *25*, 9–15. Switzer, J. A.; Kothari, H. M.; Poizot, P.; Nakanishi, S.; Bohannan, E. W. *Nature* **2003**, *425*, 490–493. Hazzazi, O. A.; Attard, G. A.; Wells, P. B. *J. Mol. Catal. A: Chem.* **2004**, *216*, 247–255.

generation" of chirality and optical activity[64] (especially in $NaClO_3$[65]), solid-state CD,[66] the chiroptics of oriented molecules,[1,2,67] the stereochemistry of adsorption to crystals,[24] or the history of stereochemistry and molecular chirality.[68]

Experimental Section

(001), (110), and (111) sections of crystals (Figure 1) were cut with a wet wire saw (South Bay Technology, model 750). They were polished to a thickness of 0.09−0.3 mm with 0.3 μm sapphire powder on a dry, ice-cooled ground glass plate in order to minimize frictional heating. Solution spectra were obtained with the cuvette sampling bench of an SI Photonics model 440 UV−vis spectrophotometer. Crystal absorption spectra were obtained by coupling the spectrometer to an Olympus BX50 transmission microscope via a 200 μm fiber optic. An Instec HS400 heating stage with a platinum resistance temperature detector was used in the racemization studies.

In order to quantify linear anisotropies, we employed the rotating polarizer technique as embodied in the Metripol microscope.[33] The application of this device to dyed crystals has been described previously.[7,34] Mechanically modulated CPL was introduced through a homemade CE imaging system that likewise has been described in this journal previously.[35]

Crystals were indexed with a Nonius KappaCCD diffractometer. Data were collected with the this diffractometer using Mo Kα radiation (λ = 0.71073 Å). Integration of intensities and cell refinement were carried out using HKL2000[69] and HKL SCALEPACK, respectively.

Commercial dye samples were analyzed with a Bruker Esquire ion-trap mass spectrometer operating in positive-ion mode. Matrix-assisted laser desorption ionization (MALDI) mass spectra were acquired on an Applied Biosystems Q-Star XL system operated in negative-ion mode. Optimum precursor ion signals in MALDI−time-of-flight (TOF) analyses, operated in reflection mode, were acquired with matrix solutions consisting of either 6200 μg/mL α-cyano-4-hydroxycinnamic acid in 56.0% acetonitrile/36.0% methanol with 0.1% trifluoroacetic acid (TFA) or 15.4 μg/mL 2,5-dihydroxybenxoic acid (Agilent Technologies) in 90% methanol with 0.1% TFA. The laser power was set to 30%, and the pulse rate was set at 20 Hz (5.2 μJ).

Acknowledgment. We thank the NSF (CHE-0349882) and the Petroleum Research Fund of the American Chemical Society for support of this research. Y.B. received a National Science and Engineering Research Council of Canada (NSERC) postdoctoral fellowship.

Supporting Information Available: Complete ref 38. This material is available free of charge via the Internet at http://pubs.acs.org.

JA1018892

(64) Lahav, M.; Leiserowitz, L. *Angew. Chem., Int. Ed.* **1999**, *38*, 2533–2536. Péres-Garcia, L.; Amabilino, D. B. *Chem. Soc. Rev.* **2007**, *36*, 941–967.

(65) Kondepudi, D. K.; Asakura, K. *Acc. Chem. Res.* **2001**, *34*, 946–954. Viedma, C. *Phys. Rev. Lett.* **2005**, *94*, 065504. Noorduin, W. L; Meekes, H.; Bode, A. A. C.; van Enckevort, W. J. P.; Kaptein, B.; Kellogg, R. M.; Vlieg, E. *Cryst. Growth Des.* **2008**, *8*, 1675–1681.

(66) Castiglioni, E.; Biscarini, P.; Abbate, S. *Chirality* **2009**, *21*, E28–E36. Kuroda, R. In *Circular Dichroism: Principles and Applications*, 2nd ed.; Berova, N., Nakanishi, K., Woody, R. W., Eds.; Wiley-VCH: Weinheim, Germany, 2000; pp 159−184.

(67) Kaminsky, W. *Rep. Prog. Phys.* **2000**, *63*, 1575–1640. Kuroda, R.; Harada, T.; Shindo, Y. *Rev. Sci. Instrum.* **2001**, *72*, 3802–3810.

(68) Lowry, T. M. *Optical Rotatory Power*; Dover: New York, 1964.

(69) Otwinowski, Z.; Minor, W. *Methods Enzymol.* **1997**, *276*, 307–326.